ATP, phosphorylation and transcription regulate the mobility of plant splicing factors

Gul Shad Ali and Anireddy S. N. Reddy*

Department of Biology and Program in Molecular Plant Biology, Colorado State University, Fort Collins, CO 80523, USA
*Author for correspondence (e-mail: reddy@colostate.edu)

Accepted 13 June 2006
Journal of Cell Science 119, 3527-3538 Published by The Company of Biologists 2006
doi:10.1242/jcs.03144

Summary

Serine-arginine-rich (SR) proteins, a family of spliceosomal proteins, function at multiple steps in the assembly of the spliceosome in non-plant systems. Limited studies with metazoan SR splicing factors (ASF/SF2 and SC35) indicated that their mobility is not dependent on ATP and phosphorylation. In addition, inhibition of transcription slightly increased their mobility. Here, we analyzed the mobility of SR45, a plant-specific SR protein with unique domain organization, and SR1/SRp34, a plant homolog of metazoan ASF/SF2, using fluorescence recovery after photobleaching (FRAP) and fluorescence loss in photobleaching (FLIP). Our results show that, in contrast to metazoan SR splicing factors, the movement of the plant SR proteins is dependent on ATP, phosphorylation and transcription. To understand the underlying mechanism for these observations, we carried out mobility analyses with the domain-deletion mutants of SR45 in ATP-depleted cells and in the presence of inhibitors of transcription or phosphorylation. Our results show that the sensitivity of SR45 to these inhibitors is conferred by an RNA-recognition motif (RRM) and the serine-arginine-rich (RS) domain 2. These results provide important insights into the mechanisms of plant SR protein movement and suggest fundamental differences in the regulation of the mobility of plant and animal SR splicing factors.

Supplementary material available online at
http://jcs.biologists.org/cgi/content/full/119/17/3527/DC1

Key words: Arabidopsis, Nuclear localization signals, Protein phosphorylation, pre-mRNA splicing, Protein mobility, SR protein

Introduction

Advances in fluorescence microscopy, together with expression of proteins tagged to fluorescent reporters, have allowed localization and analysis of the dynamics of a number of nuclear proteins in live cells (Lamond and Spector, 2003). These studies have revealed that the mammalian cell nucleus is a highly compartmentalized organelle, consisting of specialized subnuclear domains, such as Cajal bodies, promyeloid leukemia (PML) bodies, speckles and paraspeckles (Lamond and Earnshaw, 1998; Spector, 2001). The composition of different nuclear bodies appears to be very specific (Lamond and Spector, 2003). In several cases these bodies have been shown to be highly dynamic structures that continuously exchange their proteins with nucleoplasm (Misteli, 2000; Misteli, 2001; Misteli et al., 1997). Although our knowledge about similar bodies in plant cells is scarce, reports about their existence in plant nuclei are rapidly emerging (Lorkovic and Barta, 2004; Shaw and Brown, 2004), indicating that the spatial organization of the nucleus is a fundamental characteristic of all eukaryotic cells. In plant nuclei, several splicing-related proteins are distributed both diffusely in the nucleoplasm and also in concentrated foci, such as U2B, in Cajal bodies (Beven et al., 1995; Boudonck et al., 1998; Lorkovic et al., 2004).

Serine-arginine-rich (SR) splicing factors, a family of a non-snRNP proteins in the spliceosome that are known to play important roles in pre-mRNA splicing, mRNA export, RNA stability and protein translation (Huang and Steitz, 2005), are localized to speckles. In *Arabidopsis*, there are 19 non-snRNP SR splicing factors, including several plant-specific members (Kalyna and Barta, 2004; Lorkovic and Barta, 2002; Reddy, 2004), and evidence for their role in constitutive and regulated splicing of pre-mRNAs in plants is emerging (Kalyna et al., 2003; Lazar et al., 1995; Lopato et al., 1999a; Lopato et al., 1999b; Lorkovic et al., 2000). In the interphase nucleus of higher eukaryotes several of these SR proteins are present in a diffuse nucleoplasmic pool and are also concentrated in speckles (Ali et al., 2003; Docquier et al., 2004; Lamond and Spector, 2003; Lorkovic and Barta, 2004; Lorkovic et al., 2004; Tillemans et al., 2005), which correspond to interchromatin granule clusters (Fang et al., 2004; Lewis and Tollervey, 2000). Although the precise function of speckles is not known, it is thought that they are storage and/or processing and/or recycling sites of splicing factors (Lamond and Spector, 2003; Tillemans et al., 2005). The existence of twice as many SR proteins in plants as compared with animals, and the observation that some splicing factors localize to the nucleolus (Tillemans et al., 2005) indicate that certain aspects of RNA metabolism and their regulation in plants is likely to be different in animals. In addition several new plant nuclear-protein bodies, such as those containing phytochrome (Chen et al., 2003; Kircher et al., 2002) and auxin-induced proteins (Tao et al., 2005), have also been identified, suggesting the importance of nuclear compartmentalization in plants. In metazoans, several studies have provided clues about the structure, movements and nature of their resident proteins (Mintz et al., 1999; Misteli, 2001;

Misteli et al., 1997; Saitoh et al., 2004). By contrast, in plants the mechanisms that organize speckles and control the movement of their proteins are largely unknown. Initial FRAP analyses with *Arabidopsis* splicing factors suggest that, like in metazoans, plant speckles are also highly dynamic structures (Fang et al., 2004; Tillemans et al., 2005).

We have identified and characterized a plant-specific SR protein, SR45, which – unlike other splicing factors – has two serine-arginine-rich (RS) domains separated by an RRM (Golovkin and Reddy, 1999); typical SR proteins have one or two N-terminal RNA-recognition motifs (RRMs) and one C-terminal RS domain. SR45 interacts with U1-snRNP 70K protein, an SC35-like SR protein (SR33) and a LAMMER-type kinase (AFC2) (Golovkin and Reddy, 1999). In addition, baculovirus-expressed SR45 complemented the splicing-deficient S100 extract in splicing globin pre-mRNA (J. Prasad, M. Golovkin, J. Manley and A.S.N.R., unpublished results), suggesting that it is an essential splicing factor. SR45 has no homolog in animals but is ubiquitous in flowering plants, suggesting a plant-specific role for it in splicing. Because of its novelty among all SR splicing factors, we decided to gain insights into the kinetic properties of SR45 and compare them with typical plant and metazoan SR splicing factors. In animals, the SR splicing factors, ASF/SF2 and SC35, were shown to move in the nucleus independently of ATP (Kruhlak et al., 2000; Phair and Misteli, 2000). Furthermore, inhibition of transcription was shown to accelerate sequestration of ASF/SF2 splicing factor into speckles (Kruhlak et al., 2000; Phair and Misteli, 2000). Using fluorescence recovery after photobleaching (FRAP) and fluorescence loss in photobleaching (FLIP) analyses with SR45 and SR1/SRp34 (an *Arabidopsis* homolog of metazoan ASF/SF2) we show that, in contrast to metazoan SR splicing factors, the mobility of plant SR proteins is reduced by ATP-depletion and inhibition of protein phosphorylation and transcription. Using a series of deletion mutants of SR45 fused to GFP, we identified the nucleus- and speckle-targeting domains in SR45. By analyzing the mobility of these deletion mutants in cells that are either depleted of ATP, or treated with inhibitors of phosphorylation or transcription, we elucidated the role of each domain in regulating the mobility of SR45. Our findings suggest that the mechanisms that regulate the movements of plant SR proteins are different from metazoan SR proteins.

Results

We determined the relative mobility of SR45 in speckles and nucleoplasm using FRAP. Most of the SR45 recovered in the bleached areas within seconds, indicating that SR45 is a highly mobile nuclear protein (Fig. 1A,B,E). The mobility of SR45, quantified as effective diffusion coefficient (D_{eff} in μm^2 $second^{-1}$), was 1.01 μm^2 $second^{-1}$ in the nucleoplasm and 0.38 μm^2 $second^{-1}$ in the speckle (Fig. 1E, Table 1 and supplementary material Movie 1). Although the recovery of SR45 in speckles and nucleoplasm was rapid, a fraction of 9-21% remained immobile (Table 1). Similar results were obtained with SR1/SRp34 (Table 1, Fig. 2J). The D_{eff} values of

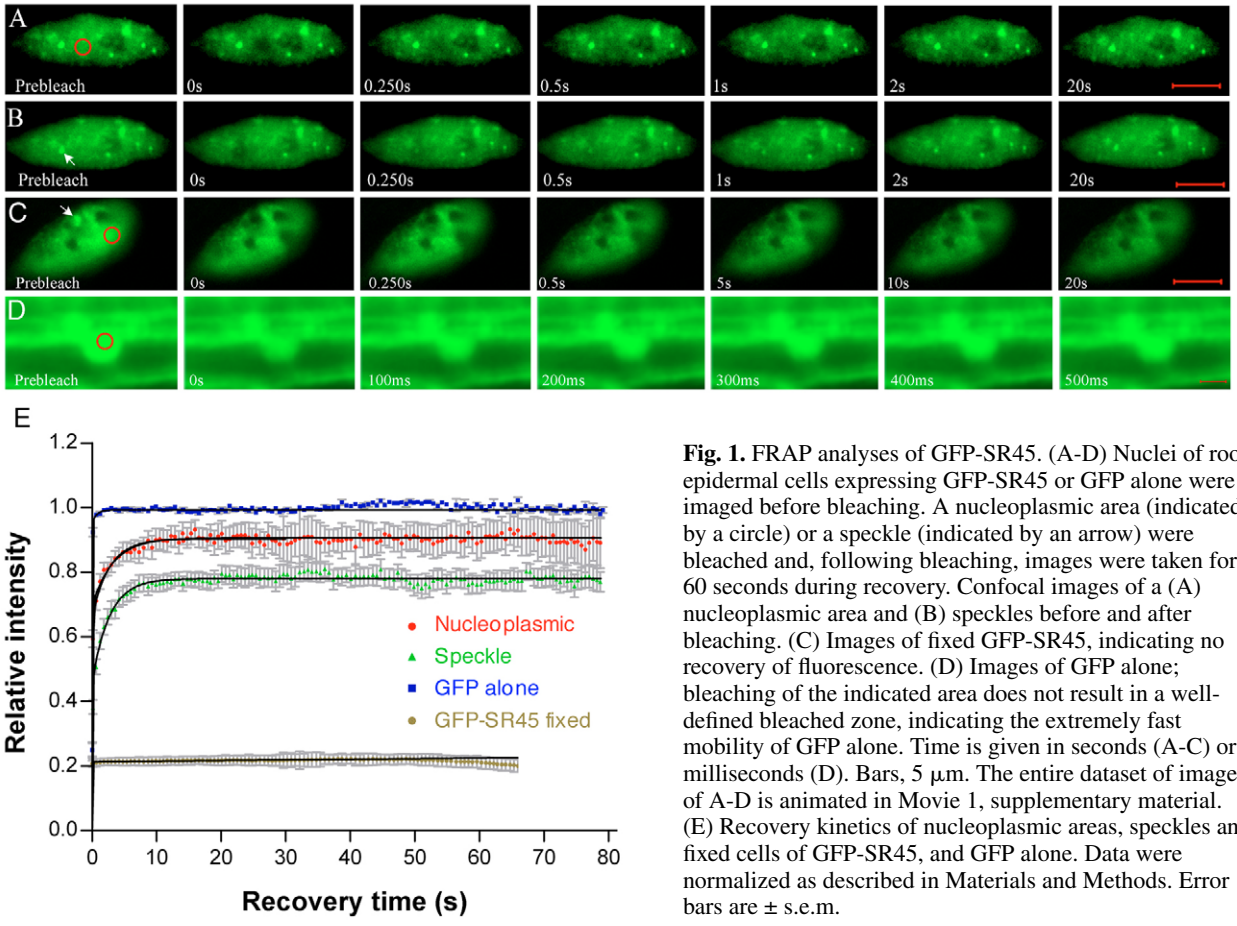

Fig. 1. FRAP analyses of GFP-SR45. (A-D) Nuclei of root epidermal cells expressing GFP-SR45 or GFP alone were imaged before bleaching. A nucleoplasmic area (indicated by a circle) or a speckle (indicated by an arrow) were bleached and, following bleaching, images were taken for 60 seconds during recovery. Confocal images of a (A) nucleoplasmic area and (B) speckles before and after bleaching. (C) Images of fixed GFP-SR45, indicating no recovery of fluorescence. (D) Images of GFP alone; bleaching of the indicated area does not result in a well-defined bleached zone, indicating the extremely fast mobility of GFP alone. Time is given in seconds (A-C) or milliseconds (D). Bars, 5 μm. The entire dataset of images of A-D is animated in Movie 1, supplementary material. (E) Recovery kinetics of nucleoplasmic areas, speckles and fixed cells of GFP-SR45, and GFP alone. Data were normalized as described in Materials and Methods. Error bars are ± s.e.m.

Table 1. D_{eff} values and mobile fractions of SR45 and SR1/SRp34 in nucleoplasm and speckles

	D_{eff} (μm^2 $second^{-1}$)	Mobile fraction (%)
GFP-SR45		
Nucleoplasmic	1.01±0.07	91±3.8
Speckle	0.38±0.18	79±4.0
Nucleoplasmic ΔATP	0.06±0.01	51±1.7
Speckle ΔATP	0.05±0.01	32±0.8
SR1/SRp34-YFP		
Nucleoplasmic	1.34±0.10	95±3.9
Speckle	0.88±0.05	82±2.5
Nucleoplasmic ΔATP	0.07±0.002	80±2.0
Speckle ΔATP	0.04±0.001	28±1.6
GFP alone	15.34±0.02	100
NLS-GFP-GUS control	10.56±0.21	100±1.37
NLS-GFP-GUS ΔATP	13.89±0.26	100±1.37

ΔATP, ATP-depletion. Values given are the mean ± s.e.m. of at least ten nuclei.

plant SR proteins were significantly smaller than that of GFP alone (15 μm^2 $second^{-1}$) or NLS-GFP-GUS (10 μm^2 $second^{-1}$), a nuclear-localized neutral protein more than twice the size of GFP-SR45 and SR1-YFP. Analysis of recovery curves indicates that first there is a rapid increase in the recovery, which is followed by a relatively slower recovery (Fig. 1E, Fig. 2J). Overall, the mobility of SR proteins is slower in the speckles than in the nucleoplasm. This was further verified by performing FLIP analysis with SR45 (Fig. 2K,M, discussed below). The loss of fluorescence in speckles was slower than in the nucleoplasm, confirming that the SR45 moves slowly in speckles (Fig. 2K). Together, these observations suggest that SR45 and SR1/SRp34 are continuously moving in the nucleus and are interacting with other nuclear components which retard their mobility.

The mobility of SR45 and SR1/SRp34 is ATP-dependent

In metazoan cells, the mobility of two SR proteins, ASF/SF2 and SC35, was shown to be ATP-independent (Kruhlak et al., 2000; Phair and Misteli, 2000). Since SR45 has a markedly different domain structure than these two proteins, we investigated whether the mobility of SR45 depends upon energy. For a meaningful comparison to metazoan SR proteins, we also performed similar analyses with SR1/SRp34, an *Arabidopsis* homolog of ASF/SF2. We depleted ATP in the cells by treating roots of GFP-SR45- or SR1-YFP-expressing *Arabidopsis* plants with the respiration inhibitor sodium azide and the glycolysis inhibitor 2-deoxyglucose, both of which are widely used and have been shown to be effective in plants (Brandizzi et al., 2002). In our experiments, ATP levels in the ATP-depleted cells were reduced by approximately 95% (supplementary material Fig. S1). Additionally, staining ATP-depleted cells with Fluorescein diacetate demonstrated that these cells remain alive during the course of the experiment (data not shown). FRAP analyses of cells that were depleted of ATP resulted in a dramatic reduction in the mobile fraction of both proteins (Fig. 2, supplementary material Movies 2 and 3). Reduced mobility of SR45 and SR1/SRp34 was observed in the nucleoplasm as well as in speckles. In the ATP-depleted cells, maximal recovery of SR45 in the speckles and nucleoplasm was 32% and 51%, respectively, compared with 79% and 91%, respectively, in controls (Fig. 2A-E, Table 1). Similarly, significant fractions of SR1/SRp34 were also rendered immobile both in the speckle and nucleoplasm (Fig. 2F-J, Table 1). Together, these results demonstrate that depletion of ATP renders a fraction of SR45 and SR1/SRp34 immobile. Similarly, D_{eff} values of both proteins were also significantly reduced in the ATP-depleted cells. Replacing the ATP-depleted culture medium with regular medium restored the high mobility, indicating that the ATP-dependent immobilization of SR45 is reversible (data not shown). Furthermore, ATP-depletion for 15 minutes also resulted in reduced mobility, further indicating that the reduced mobility is due to ATP depletion. ATP-depletion had no effect on the mobility of neutral GFP alone and on a nuclear localized GFP-GUS (NLS-GFP-GUS) that is twice the size of SR45 (Table 1). Fig. 2E shows that a fraction of SR45, both in speckles and nucleoplasm (represented by a steep rise in the curves from 0 seconds to ~0.5 seconds), displayed faster mobility, whereas the rest exhibited very slow mobility, reflected by a very slow rise in the curves from 0.5 to 80 seconds (there was no further rise in the curve after 80 seconds for up to 10 minutes, data not shown).

To confirm the results obtained with FRAP analyses, we conducted FLIP analyses. We repeatedly bleached a defined area at one end of the nucleus and monitored the loss of fluorescence in an unbleached part of the nucleus. In untreated controls, FLIP analyses clearly showed that fluorescence in the unbleached area is reduced gradually until it disappears almost completely, indicating that GFP-SR45 in the bleached zone is exchanged with the fluorescent GFP-SR45 from the unbleached area, suggesting a high mobility of the GFP-SR45 (Fig. 2K, bottom nucleus, and Fig. 2M; supplementary material Movie 4). In the ATP-depleted nuclei, however, very little loss in the unbleached area was observed (Fig. 2L, bottom nucleus, and Fig. 2M; supplementary material Movie 4). These observations corroborated the FRAP analyses. Taken together, these data indicate that the movement of SR45 and SR1/SRp34, in contrast to SR proteins in metazoan (Kruhlak et al., 2000; Phair and Misteli, 2000), depends upon ATP.

Inhibition of protein phosphorylation and transcription retards the mobility of SR45 and SR1/SRp34

We have shown previously that inhibition of transcription and phosphorylation sequestered SR45 to large speckles (Ali et al., 2003). Similarly, inhibition of transcription led to altered localization pattern also of other plant SR proteins (Fang et al., 2004; Tillemans et al., 2005). These analyses, however, did not address how these inhibitors affected the movement of individual SR45 and SR1/SRp34 molecules. To gain insights into these processes we performed FRAP analyses on roots treated with the transcription inhibitor actinomycin D or the protein kinase inhibitor staurosporine. Both these inhibitors significantly decreased the mobility of SR45 and SR1/SRp34 (Fig. 3 and supplementary material Movie 5). The D_{eff} values of SR45 were reduced by four times by both treatments, whereas the D_{eff} values of SR1/SRp34 were reduced by 14 times by staurosporine and eight times by actinomycin D. With the exception of actinomycin D treatment of SR1/SRp34, all other treatments also significantly reduced the mobile fractions of SR45 and SR1/SRp34 (Fig. 3D,H,I). These observations suggest that the mobility of SR45 and SR1/SRp34 is regulated by transcription and protein phosphorylation.

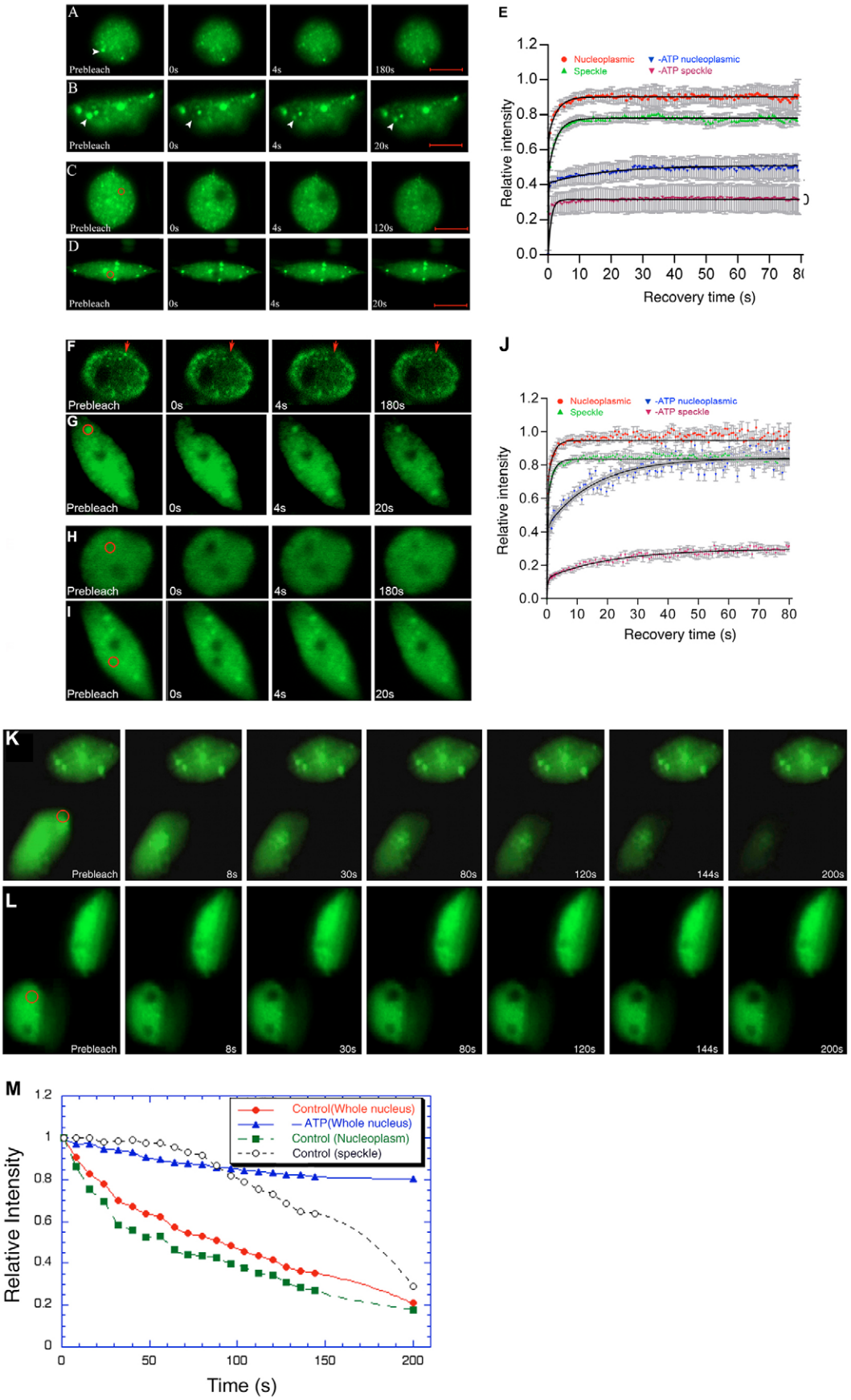

Fig. 2. See next page for legend.

Table 2. Summary of D_{eff} values and mobile fractions of the GFP-tagged SR45-deletion mutants after treatment with different inhibitors

GFP-fusions (predicted molecular mass in kD)	Control		ΔATP		Staurosporine		Actinomycin D	
	D_{eff}	Mobile fraction (%)	D_{eff}	Mobile fraction (%)	D_{eff}	Mobile fraction (%)	D_{eff}	Mobile fraction (%)
RS1 (38)	1.82±0.04	100±1.1	1.01±0.01	100±1.4	0.75±0.02	97±1.6	1.57±0.04	100±0.1
RRM (36)	0.80±0.08	97±2.2	0.03±0.01	15±6.3	0.29±0.02	73±5.7	0.94±0.08	92±1.0
RS2 (56)	0.60±0.03	96±3.4	0.08±0.004	78±1.5	0.10±0.003	84±3.6	0.56±0.04	84±1.6
RS1+RRM (46)	1.62±0.04	100±1.3	0.05±0.003	15±2.4	0.41±0.01	100±3.1	1.26±0.05	97±3.1
RRM+RS2 (63)	1.32±0.05	31±1.4	0.12±0.03	8±0.5	0.11±0.01	18±0.2	0.20±0.06	25±1.7

Free predicted diffusion (μm^2 $second^{-1}$) in the absence of binding are: GFP-RS1, 13.6 μm^2 $second^{-1}$; GFP-RRM, 13.8 μm^2 $second^{-1}$; GFP-RS2, 11.9 μm^2 $second^{-1}$; GFP-RS1+RRM, 12.7 μm^2 $second^{-1}$; GFP-RRM+RS2, 11.5 μm^2 $second^{-1}$.

ΔATP, ATP-depletion. Values given are the mean ± s.e.m. of at least ten nuclei.

Subcelluar localization and mobility of SR45 deletion mutants

Among the *Arabidopsis* SR splicing factors, SR45 has a more complex but well-defined modular domain structure. It consists of an N-terminal RS domain, a middle RRM domain and a C-terminal RS domain (Fig. 4A). The RS domains consist of serine-arginine dipeptide repeats that are thought to mediate protein-protein interactions, whereas the RRM domain consists of an 80-amino-acid-long RNA-binding domain that is known to interact with RNA sequences and often determines specificity in binding RNA sequences. To determine the role of each of these domains in subcellular localization and mobility of SR45, we generated several deletion mutants fused to GFP (Fig. 4A). Each of the GFP-tagged mutants and full-length SR45 were expressed in *Arabidopsis* mesophyll protoplasts and examined with a confocal microscope. Full-length GFP-SR45 localized exclusively to the nucleus in a typical diffused and speckled pattern (Fig. 4B), in agreement with our previous observations in transgenic *Arabidopsis* plants (Fig. 1). With the deletion mutants, several obvious differences in the localization pattern were observed, which are summarized in Fig. 4A and illustrated in Fig. 4B. RS1 was predominantly localized in the nucleus but a very faint signal was also present in the cytoplasm, probably because of the presence of a single weaker NLS in this domain (Fig. 4B). RRM alone, like GFP, was present both in the cytoplasm and nucleus, suggesting absence of any subcellular targeting signals. Mutants that consisted of RS2 alone or of RS2 in combination with RRM were exclusively found in the nuclei, suggesting that the nuclear localization signals are present in the RS2 domain. The mutant that consisted of RS1 and RRM but lacked RS2 was present mostly in the nucleus but a sizeable fraction was also present in the cytoplasm. Mutants that localized to the speckles contained RS2 either alone or in combination with RRM, indicating that the speckle-targeting and speckle-retention signals are located in the RS2 domain (Fig. 4B). RS1 and RRM, either alone or together, were exclusively distributed in a diffused pattern, indicating that these domains by themselves are not sufficient for speckle targeting (Fig. 4B). In summary, these results revealed that both RS1- and RS2-domains contain nuclear localization signals that function independently of each other. The speckle-targeting or speckle-retention signals are exclusively located in the RS2 domain, which is necessary and sufficient for speckle localization. The RS1 and RRM domains, however, are neither necessary nor sufficient for speckle targeting.

The presence of RS and RRM domains in SR45 indicates that it interacts with both proteins as well as RNA and, therefore, the reduced recovery in FRAP – as described above – results from its interaction with multiple components in the nucleus. The domain-deletion mutants described above represent different parts of SR45 and probably have different interaction properties. This allowed us to dissect the kinetic properties of each domain of SR45 using FRAP analyses and, hence, determine the relative contribution of each domain to the overall mobility of SR45. Based on the relationship, $D\alpha M^{-1/3}$ (diffusion is inversely proportional to the cubic root of mass) and the experimental D value of GFP alone (see Materials and Methods), the predicted free-diffusion coefficients (D) for full-length SR45 and the deletion mutants in the absence of binding, were calculated (Sprague et al., 2004) (Table 2). These values were used in the equation described in Materials and Methods to generate simulation curves that reflect free diffusion. These simulation curves are displayed as red curves in graphs in Fig. 5A-E. Curves that best fit the experimental data are shown as black lines superimposed on the data points. The D_{eff} values, defined as slowed diffusion

Fig. 2. FRAP and FLIP analyses reveal that the mobility of SR45 and SR1/SRp34 depends upon ATP. (A-D,F-I,K-L) A speckle (arrowhead) or a defined nucleoplasmic area (circle) in control or ATP-depleted cells was imaged before bleaching and during recovery for the time indicated. (A-D,F-I) Subsets of confocal images of a speckle (arrows in F) in ATP-depleted cells (A) SR45 and (F) SR1/SRp34, and control cells (B) SR45 and (G) SR1/SRp34. The entire set of time-lapse images of SR45 is animated in Movie 2, supplementary material. Subsets of confocal images of a nucleoplasmic area (circle) in ATP-depleted cells (C) SR45 and (H) SR1/SRp34, and control cells (D) SR45 and (I) SR1/SRp34. The entire time-lapse series of images for SR45 is animated in Movie 3, supplementary material. Bars, 5 μm. (E,J) Quantification of recovery kinetics of a speckle or a nucleoplasmic area in ATP-depleted cells of (E) SR45 and (J) SR1/SRp34. Curves shown are averages of at least ten nuclei in three different experiments. Error bars are ± s.e.m. (K,L) Subset of images of FLIP analyses of SR45. In each panel two adjacent nuclei of GFP-SR45 cells, either (K) untreated or (L) treated with NaN_3 and 2-deoxyglucose are shown. A defined area (circle) in the lower nucleus of each panel was repeatedly bleached and photographed at the indicated times. The upper nucleus was not bleached and served as a reference for the normalization of fluorescence intensities. Very little loss of fluorescence in the unbleached zone of ATP-depleted nuclei indicates that the movement of GFP-SR45 is dependent upon ATP. The entire dataset of K and L is animated in Movie 4, supplementary material. (M) Quantitative FLIP analyses of the control and ATP-depleted GFP-SR45. Data presented are representative of five nuclei.

resulting from binding full-length or deletion mutants of SR45, were determined from the fit to the experimental FRAP data and are summarized in Table 2. A comparison of the D_{eff} values of the single-domain-containing mutants (i.e. RS1, RRM and RS2) suggests that the RS1 domain interacts with other components in the nucleus to a lesser extent than RRM and RS2 (Table 2). Interestingly, none of the combinations reduced the mobility in an additive fashion as would be expected if each

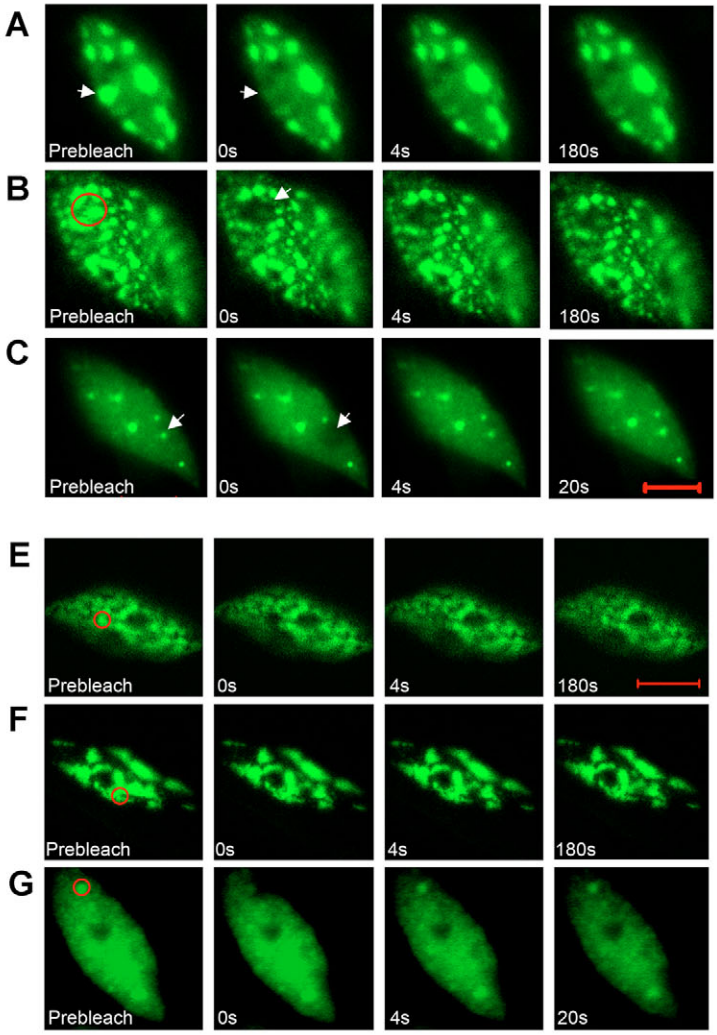

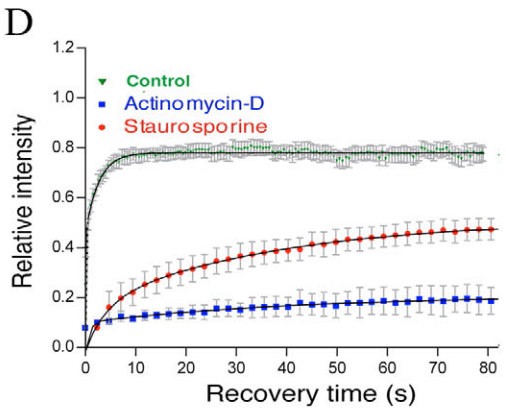

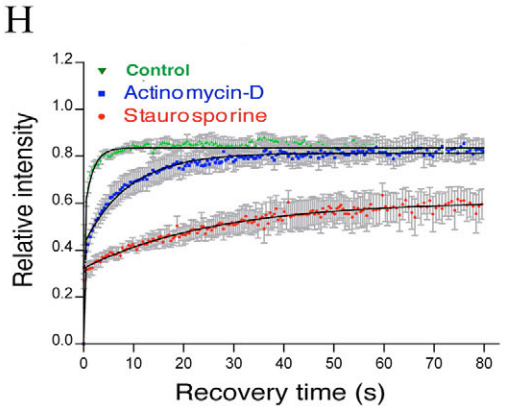

I

	SR45		SR1	
	D_{eff}	% Mobile	D_{eff}	% Mobile
Control	0.38±0.18	79±4.0	0.88±0.05	82±2.5
Actinomycin-D	0.09±0.01	23±0.4	0.11±0.003	82±2.6
Staurosporine	0.1±0.01	54±3.6	0.06±0.004	61±3.6

Fig. 3. FRAP analyses of SR45 and SR1/SRp34 movement in cells treated with inhibitors of transcription or protein kinases. (A-C,E-G) Subsets of confocal images of epidermal nuclei treated with actinomycin D (A) SR45 and (E) SR1/SRp34, staurosporine (B) SR45 and (F) SR1/SRp34), and control (C) SR45 and (G) SR1/SRp34. A defined area or speckle (marked by a circle or arrow, respectively) was imaged before and after bleaching. The entire data set of A-C was animated and is presented in Movie 5, supplementary material. (D,H) Recovery kinetics of SR45 (D) and SR1/SRp34 (H) in nuclei not treated (control) or treated with actinomycin D or staurosporine. Curves are averages of at least ten nuclei of two experiments. Error bars are ± s.e.m. (I) Diffusion coefficients of SR45 and SR1/SRp34 in control and treated cells. Values are the mean ± s.e.m. of at least ten cells.

of the domains were acting independently (Table 2). These results underline the complexity of interaction of various domains in regulating the mobility of full-length SR45.

Mobile and immobile fractions were also calculated for each deletion mutant. The immobile fractions are graphically displayed as the differences between the plateaus of red (complete recovery) and black (maximal recovery) curves (Fig. 5A-E) and are presented in Table 2. Mutants that contain RS1 alone or RS1 together with RRM recovered completely, without a immobile fraction, whereas deletions consisting of RRM or RS2 alone had some immobile fraction; however, those were considerably smaller than for full-length SR45. Most notably, the deletion mutant containing RRM and RS2 together (lacking RS1) had an unusually large immobile fraction (69%), indicating that RS1 plays an important role in regulating mobility of SR45. In summary, these data suggest that each SR45 domain can interact with nuclear components independently of other domain(s) and that, in general, absence of a domain increases the mobility of SR45, presumably by decreasing its frequency of interaction with other components.

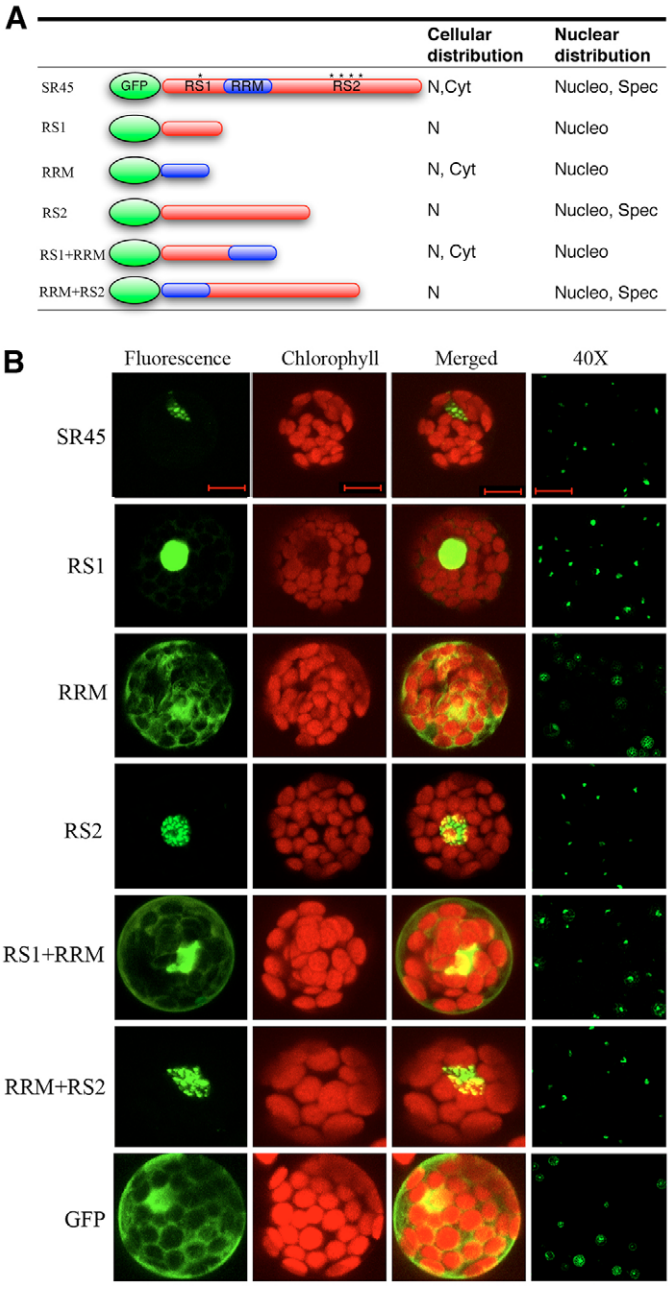

Role of SR45 domains in conferring sensitivity to ATP depletion, to inhibitors of protein phosphorylation and to transcription

In an effort to determine the SR45 domain(s) that are responsible for the observed sensitivity of full-length SR45 to ATP, staurosporine and actinomycin D, we performed FRAP analyses with each deletion mutant after treatment with the inhibitors. Sensitivity was assessed by changes in the subcellular localization pattern, D_{eff} and mobile fractions. The results are summarized in Table 2 and are graphically presented in Fig. 5. First, ATP depletion did not change the distribution of RS1; it remained in a diffused pattern like in control (Fig. 5, panel A). By contrast, a substantial fraction of RRM, which has a molecular weight comparable to RS1, concentrated in numerous foci in the cytoplasm (Fig. 5, panel B). In addition, a substantial fraction (82%) of RRM in these foci was rendered immobile (Fig. 5, RRM; Table 2). Second, despite being similar in size and with similar diffusion properties under control conditions, RS1 and RRM had different mobile fractions in ATP-depleted cells, (100% and 15%, respectively) and a disproportionate reduction in D_{eff} (1.8× for RS1 and 27× for RRM) (Fig. 5 and Table 2). Third, the RS1-RRM domain, although smaller than RS2 (46 kD vs 56 kD), had a significantly higher immobile fraction than the RS2 domain (Fig. 5, Table 2). These observations suggest a scenario where ATP plays an active role in the mobility of SR45 and, therefore, the observed reduced mobility of SR45 in ATP-depleted protoplasts does not result from non-specific general perturbation of the cellular environment. Also, we conclude that ATP sensitivity is primarily conferred by RRM and RS2 because the deletion mutants having these domains, either alone or in combination with other domains, still maintained a strong response to ATP in their mobility properties, whereas the presence of RS1 alone had a very small effect (Fig. 5, Table 2).

Fig. 4. Localization of full-length SR45 and deletion mutants of SR45 fused to GFP. (A) Schematic diagram of the GFP-tagged SR45 deletion mutants. RS1 and RS2, arginine-serine-rich domain 1 and domain 2, respectively; RRM, RNA-recognition motif. Asterisks on full-length GFP model indicate location of predicted nuclear localization signals (NLS). Table on the right side summarizes the subcellular and subnuclear localization of GFP-tagged full length and deletion mutants of SR45. N, Nuclear; Cyt, Cytoplasmic; Nucleo, Nucleoplasmic; Spec, Speckle. (B) *Arabidopsis* mesophyll protoplasts were transiently transfected with vectors expressing the indicated GFP-tagged SR45 mutant and examined by confocal microscopy. Shown are single confocal optical sections. Fourth column of panels displays the expression of GFP-fusions in several protoplasts in a single-view field at low magnification (40×); bar, 100 μm. First, second and third column of panels show fluorescence images, chlorophyll autofluorescence images and their respective merged images (as indicated above each panel); bars, 10 μm. As expected, full-length SR45 localized in a speckled pattern in the nucleus. The rest of the mutants displayed a range of distributions, summarized in A.

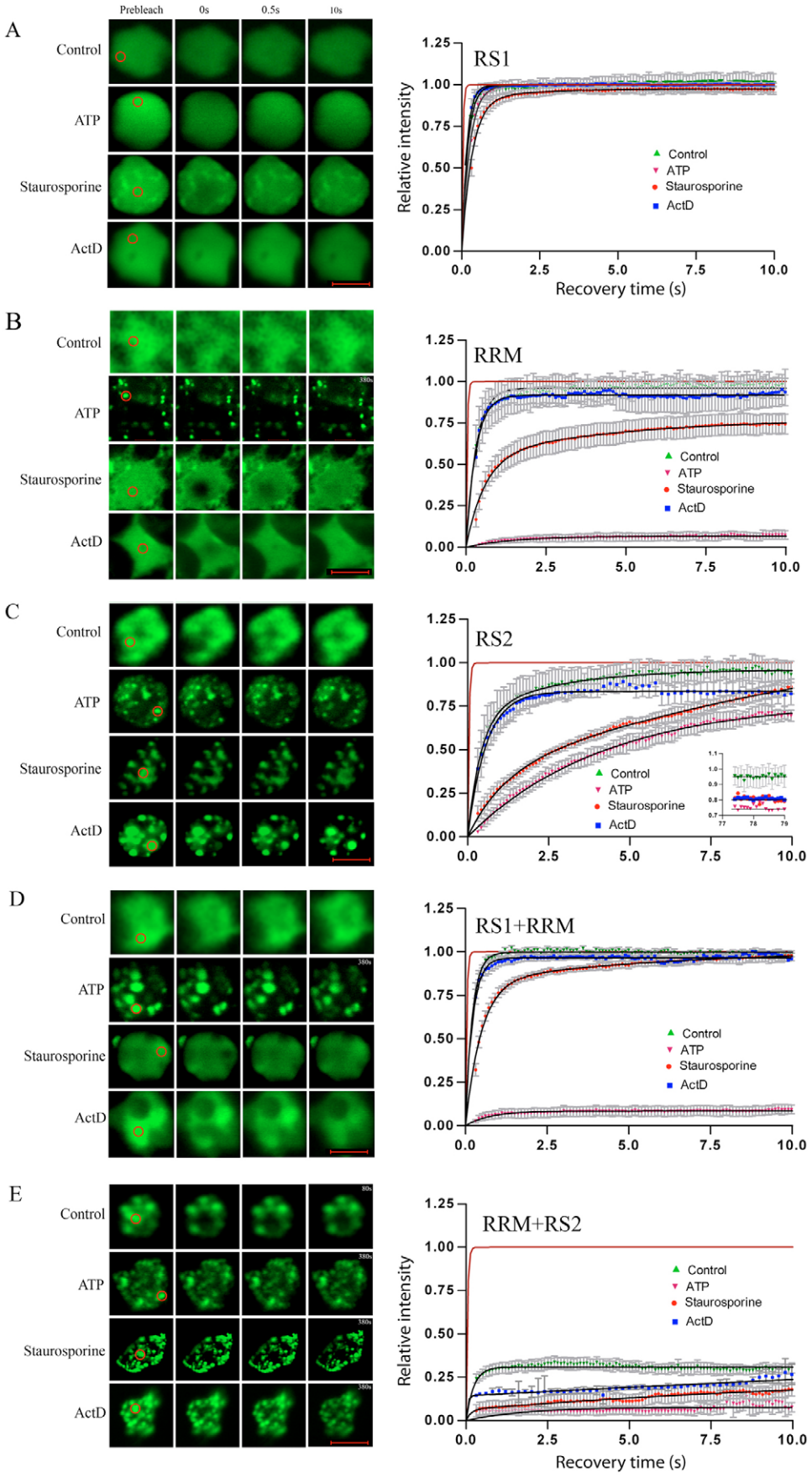

Fig. 5. See next page for legend.

In mammalian cells, substrate specificity and interaction, and subcellular localization of SR proteins is mediated by the phosphorylation of the RS domain. The presence of two RS domains in SR45 makes it interesting to determine the effect of phosphorylation of these two domains on SR45 mobility. In the kinase-inhibited cells, domains that contained RS2 were redistributed to irregular-shaped speckles in a fashion similar to full-length SR45 (Fig. 5, panel C). The RS1 domain, either alone or in combination with RRM, exhibited altered redistribution in the form of faint, irregularly shaped speckles on the background of a strong diffused pattern (Fig. 5, panel A and D). The subcellular distribution of RRM domain alone was not affected by kinase inhibition. FRAP analyses with these domain deletions showed that staurosporine treatment significantly reduced mobility of all deletion mutants except RS1 (Fig. 5, Table 2). RS1 alone was marginally affected, whereas RS2 was very strongly affected. Based on these observations, we conclude that RRM and RS2 are the main domains that confer sensitivity to staurosporine, whereas RS1 plays a role in redistribution of SR45 in response to staurosporine.

To examine the role of each domain in determining specificity to transcription inhibition, all deletion mutants were analyzed for their subcellular localization and for their mobility after treatment with actinomycin D. Under transcriptional inhibition conditions, the subcellular localization pattern of most of the deletion mutants, except RS2, did not show any obvious shift in localization pattern. RS2 showed rounding of speckles. This indicates that the effect of actinomycin D is mediated by the RS2 domain. Similarly, the D_{eff} value of any domain alone was not markedly affected by actinomycin D (Fig. 5E, RRM+RS2; Table 2). In combination, however, RRM and RS2, exhibited reduced mobility very similar to full-length SR45. In this deletion mutant and in RS2 alone, the mobile fractions were also moderately decreased (Table 2). These observations suggest that, full-length SR45, or at least the presence of both RRM and RS2, is necessary for a transcription-dependent change in the mobility of SR45.

Discussion

Mobility properties for several typical plant and metazoan SR proteins are known (Fang et al., 2004; Phair and Misteli, 2000; Tillemans et al., 2005). SR45 – despite having a domain organization that is different from typical SR proteins – like typical SR proteins, moves very slowly compared with a neutral protein of similar size. This indicates that the movement of SR45 is reduced by its interaction with other components, such as U1-70K, SR33 and AFC2, which in turn are parts of larger spliceosomal complexes (Golovkin and Reddy, 1999; Reddy, 2004; Reddy, 2001), thus impeding free diffusion of SR45 in the nucleus. Recently, FRAP analyses with *Arabidopsis* SR proteins RS31 (Tillemans et al., 2005), SR1/SRp34 and SR33 (Fang et al., 2004) revealed that these proteins had recovery half-times of ~5.6 seconds (atRSp31) and ~2.5 seconds (SR1/SRp34 and SR33), which are considerably greater than those of GFP alone or NLS-GFP-GUS. Similarly, a D_{eff} value of 0.24 μm^2 $second^{-1}$ for the metazoan SF2/ASF protein was reported (Phair and Misteli, 2000). Overall, SR45 had kinetic properties that are similar to other plant SR proteins, albeit with a slightly slower diffusion, probably resulting from the addition and regulation of RS1. We also observed that SR45 and SR1/SRp34 in the speckles had significantly slower diffusion than in the nucleoplasm (Fig. 1E and Table 1), suggesting that binding partners of SR proteins are in excess in speckles.

The mobility of SR45 and SR1/SRp34 requires ATP

Using sodium azide and 2-deoxyglucose, two extensively used inhibitors of ATP in metazoans and plants (Brandizzi et al., 2002; Phair and Misteli, 2000), we show that the mobility of SR45 and SR1/SRp34 depends upon ATP. Previously, it has been shown that depletion of ATP has either no effect or slightly increased the movement of human ASF/SF2 (Kruhlak et al., 2000; Phair and Misteli, 2000). Our results clearly show that the mobility of SR45 and SR1/SRp34, an *Arabidopsis* homolog of ASF/SF2, is reduced by ATP, suggesting that the mobility of plant SR proteins is regulated in a manner different from metazoan splicing factor SF2/ASF. By using GFP-tagged RNA-binding proteins, which are different from SR proteins, or by directly examining mRNA with fluorescent probes, it was shown that the diffusion of mRNPs is reduced by ATP depletion (Calapez et al., 2002; Molenaar et al., 2004; Vargas et al., 2005). This reduced diffusion was associated with a global change in the nuclear environment (Shav-Tal et al., 2004). Although we do not entirely rule out a similar possibility for plant SR proteins, several observations in this study indicate that ATP depletion has a specific effect on the mobility of plant SR proteins. First, differential effects on the subcellular localization of SR45 deletion domains demonstrate that ATP exerts its effect through specific domains instead of a very general change in the surroundings. Second, a global nuclear rearrangement would be expected to restrict the mobility of other nuclear protein too. Our analyses show that ATP depletion had no effect on the mobility of the nuclear localized NLS-GFP-GUS fusion protein, which is twice as large as SR45. However, being neutral, one can argue that NLS-GFP-GUS is not present in large enough complexes to be impeded by smaller size ‘pores’ presumably generated by the rearrangement of chromatin by ATP depletion (Shav-Tal et al., 2004). Table 2 shows diffusion coefficients and molecular masses of individual domains of SR45. If the reduced mobility is merely due to global change in the nuclear environment, we would expect a proportionally similar effect of ATP-depletion on the mobility of these domains. On the contrary, however, we saw a disproportionate effect of ATP-depletion on these deletion mutants. These observations, together with the finding that the neutral proteins (GFP and NLS-GFP-GUS) are not

Fig. 5. Contribution of various domains to SR45 mobility and subcellular localization under control conditions, and after treatment with various inhibitors. (A-E) Optical sections from representative FRAP images of protoplasts expressing a deletion mutant. Circles indicate regions that were bleached (A) RS1; (B) RRM; (C) RS2; (D) RS1+RRM; (E) RRM+RS2. Bars, 10 μm. Quantitative FRAP analyses of the SR45-deletion mutants are shown to the right of each set of images. Error bars are ± s.e.m. of at least ten cells. Inset in C shows final recovery levels. Curves in red lines give the theoretical curves a protein of the molecular mass equivalent to the GFP-fusion protein would follow in the absence of any binding (see Materials and Methods). Curves in black give the best-fit curves to the experimental data of an exponential equation determined by the least-square method.

substantially effected, suggest that ATP specifically affects the mobility of SR45 through specific domains. The recovery in a bleached region results from the exchange of bleached molecules with fluorescent molecules from the surrounding areas. This could be interpreted as repeated dissociation and reassociation of SR proteins to its binding sites. The slowed recovery in the ATP-depleted cells indicates that binding and unbinding of SR proteins depends upon ATP. Since ATP is required for the rearrangements of spliceosomal complexes during splicing, in the absence of ATP, these proteins probably do not readily dissociate from larger complexes; and this is manifested in the form of retarded mobility of SR proteins. ATP-depletion might also cause hypophosphorylation of SR45 and SR1/SRp34, which – like in animal SR proteins (Xiao and Manley, 1997) – may affect its interaction with other proteins and RNA, and consequently its movement for recruitment to sites of transcription (Misteli and Spector, 1999). However, differential effects of ATP and staurosporine on the subcellular localization of full-length SR45 (Figs 2 and 3) and several deletion mutants, such as RRM and RS2 (Fig. 5B,C), suggest that mechanisms other than phosphorylation or in addition to phosphorylation are involved in regulating plant SR-protein mobility by ATP.

The recovery of SR45 and SR1/SRp34 is reduced by inhibition of protein phosphorylation and transcription

Since SR45 and SR1/SRp34 play roles in splicing and are phosphoproteins, their change in mobility and localization patterns in response to transcriptional and phosphorylation inhibition provides an important clue to their regulation. The effect of staurosporine on the mobility of SR45 and SR1/SRp34 does not appear to be common to all SR proteins, because this inhibitor does not affect the movement of ASF/SF2 (Kruhlak et al., 2000). In our analyses, even a 25 times lower concentration of staurosporine than that reported by Kruhlak et al. (Kruhlak et al., 2000), drastically reduced the movement of SR45 and SR1/SRp34. The reduced mobility of SR45 and SR1/SRp34 in speckles after kinase inhibition probably results from their failure to release from speckles in a hypophosphorylated state. This explanation is supported by the observation that SF2/ASF is recruited to splicing sites in a hyperphosphorylated state. In addition, disrupting the phosphorylation of SF2/ASF by mutating the RS dipeptides to RG-dipeptides abolished its recruitment to active transcription sites (Misteli et al., 1998). Analyses with domain-deletion mutants of SR45 after protein-kinase inhibition showed that, primarily the RS2 and RRM domains and, to some extent, the RS1 domain respond to phosphorylation. There are 12 and 16 RS-SR dipeptides in the RS1 and RS2 domains, respectively, which might be phosphorylation sites. These observations are consistent with a model where RNA-substrate-specificity and -interaction, and subcellular localization of SR proteins is mediated by the phosphorylation of the RS domain (Misteli et al., 1998). The effect of kinase inhibition on RRM is probably because of the effect of phosphorylation on complexes the RRM interacts with. These observations and the findings that serine phosphorylation of SR proteins is required for their recruitment to sites of transcription (Misteli et al., 1998) and that inhibition of transcription causes enlargement of speckles (Ali et al., 2003; Docquier et al., 2004; Tillemans et al., 2005; Zeng et al., 1997) indicate that movement of SR proteins depends upon transcription and phosphorylation. In animal cells, several observations suggest that speckles are the sites of storage and/or processing of the splicing-associated proteins (Lamond and Spector, 2003). FRAP analyses performed with SR45 and SR1/SRp34 suggest that, like their metazoan counterparts, plant SR proteins are continuously exchanged between speckles and nucleoplasm. After transcriptional or protein phosphorylation inhibition, SR45 and SR1/SRp34 do not dissociate readily from their interacting partners in the speckle and therefore do not leave the speckle efficiently or, like metazoan SR-splicing factors, phosphorylation is a pre-requisite for their release from speckles (Misteli et al., 1998). Further, changes in the phosphorylation state of SR proteins are shown to affect their subnuclear distribution and activity in splicing (Misteli et al., 1997; Sacco-Bubulya and Spector, 2002; Sanford and Bruzik, 1999; Zeng et al., 1997). Overexpression of a LAMMER-type protein kinase (CLK/STY) and SR protein kinase redistributed SR proteins to a diffuse nucleoplasmic pool (Colwill et al., 1996; Sacco-Bubulya and Spector, 2002), whereas expression of an inactive mutant form of CLK/STY kinase caused increased accumulation of SR proteins in speckles (Sacco-Bubulya and Spector, 2002). These observations, together with the inhibition of peripheral movement of ASF/SF2 as well as sequestration of SR45 and SR1/SRp34 into speckles after treatment with staurosporine (Ali et al., 2003; Misteli et al., 1997), indicate that the intranuclear distribution of SR proteins depends upon their phosphorylation status. We have shown previously that, in vitro, SR45 interacts with and is phosphorylated by AFC2, a LAMMER-type kinase that might regulate the mobility of SR45 and probably SR1/SRp34 (Golovkin and Reddy, 1999). The reduced movement of SR45 in actinomycin-D- and staurosporine-treated cells indicates that the mobility of GFP-SR45 depends upon transcription and phosphorylation. The slightly increased mobility of SF2/ASF in transciptionally inhibited cells was explained as diminished population of the substrate RNA transcripts (Phair and Misteli, 2000) or simply as the redistribution of non-RNA-binding sites from nucleoplasm to speckles (Kruhlak et al., 2000). Our results suggest that animal and plant splicing factors are differentially affected by the status of transcription. A possible explanation for our results is that in the absence of transcription and, hence splicing, splicing factors are not recruited to active transcription sites. Instead, they remain tightly bound to their binding sites in the speckles, accounting for their retarded mobility.

The RS2 domain is necessary and sufficient for the formation of SR45 speckles

Using deletion mutants consisting of different domains of SR45 fused to GFP, we have identified nuclear localization and subnuclear distribution signals in SR45. Primary sequence analyses with predictNLS (Cokol et al., 2000), PROSITE scan Release 19.11 (http://www.expasy.org/prosite/) and PSORT (http://www.psort.org/) indicated that there are several putative NLS in the RS1 and RS2 domains. Consistent with predictions, mutants consisting of RS1 or RS2 localized to nuclei, albeit at different strengths (Fig. 4). The RS2 domain is necessary and sufficient for speckle targeting. In previous studies, RS

domains of *Arabidopsis* atRSp31 and atRSZp22 (Tillemans et al., 2005), *Drosophila* suppressor-of-white-apricot (SWAP) (Li and Bingham, 1991) and transformer (Tra) (Hedley et al., 1995), and of the human SC35 and SRp20 (Caceres et al., 1997), have been shown to direct these proteins to speckles. The speckle-targeting motif in these proteins was proposed to be a stretch of three or four arginine or lysine residues followed by RS dipeptides (Hedley et al., 1995). In agreement with these studies, the RS2 domain of SR45 has one such minimal motif (RRRSR; aa 331-335). The RS1 domain of SR45, on the other hand, is neither necessary nor sufficient for speckle formation. With the exception of SR45, in all of the known typical SR splicing factors the RS domain is always located at the C-terminus of a protein (Graveley, 2000; Lorkovic and Barta, 2002; Reddy, 2004). The SR45 RS1 domain is unusually located at the N-terminus of SR45 and, therefore, might not be mediating speckle targeting. The RRM of several other nuclear proteins, such as polypyrimidine tract-binding (PTB)-associated splicing factor (PSF) (Dye and Patton, 2001) and ASF/SF2 (Caceres et al., 1997), have also been shown to have speckle-targeting signals. The expression of only the RRM of SR45 (this study), atRSp31 and atRSZp22 (Tillemans et al., 2005) did not reveal any speckles, indicating that, in contrast to PSF and ASF/SF2, the RRM of these plant SR proteins by itself does not carry any signals for speckle targeting, and points to differences in their regulation of subcellular localization.

In summary, regulation of the intranuclear localization and mobility of SR45 by ATP, transcription and protein phosphorylation on one hand, and by various protein domains on the other hand, suggests that its activity is regulated spatially and temporally by complex interactions with other proteins and RNAs. The differences in the regulation of mobility of SR45 and metazoan SR proteins (ASF/SF2 and SC35) suggest that not all SR proteins exhibit similar dynamics, and that such differences probably have important implications in pre-mRNA splicing.

Materials and Methods

Preparation of plant material for confocal microscopy

Transgenic seedlings expressing GFP-SR45 or SR1/SRp34-YFP (Fang et al., 2004) were grown on agar-solidified Murashige and Skooge (MS)-medium plates (MS salts, 10% sucrose and 0.8% Phytagar) and grown under a 12 hour-12 hour dark-light cycle at 24°C (Ali et al., 2003). A root tip (2-4 mm) from 7-day-old to 10-day-old seedlings that were treated as described below was mounted in a homemade perfusion chamber that allowed ventilation and change of inhibitor-containing solutions during the course of confocal microscopy. *Arabidopsis* plants expressing GFP alone or a nucleus-localized chimeric protein of GFP or NLS-GFP-GUS were used as controls.

GFP-tagged deletion mutants of SR45 and transient protoplast transfections

GFP-SR45-deletion fusion constructs depicted in Fig. 4 were made as follows: the N-terminal RS1 domain (aa 1-98), the RRM domain (aa 99-172), RS2 domain (aa 173-414), RS1+RRM domain (aa 1-172), RRM+RS2 (aa 99-414) and RS1+RRM+RS2 (aa 1-414, full length) were PCR-amplified with forward and reverse primers containing *Sal*I and *Xma*I restriction sites, respectively, and cloned at the 3′ end of GFP in pGFP II (GA5), a plant-expression vector. All fusion constructs were verified by sequencing. Each construct was transiently expressed in *Arabidopsis* mesophyll protoplasts using a standard polyethylene glycol (PEG) transfection protocol (Abel and Theologis, 1994). Briefly, protoplasts were isolated from tissue-culture-grown 4-week-old plants using 2% cellulase (Onozuka R-10) and 0.2% macerozyme (R-10, Yakult Hansha Co, Japan) in W5 medium (154 mM NaCl, 125 mM $CaCl_2$, 5 mM KCl and 2 mM MES). Approximately 2×10^6 protoplasts were transfected with 10 μg plasmid DNA in 40% PEG for 30 minutes. PEG was removed by diluting the protoplasts with W5 medium followed by centrifugation at 100 ***g*** for 2 minutes. The protoplast pellet was resuspended in W5 medium with or without 5 mM glucose in the ATP-depletion experiments, and incubated in a 6-well plate in the dark at 22°C for 18 hours. A 50-μl aliquot of the expressing protoplasts was transferred to a glass-slide, covered with an O-type (30-70 μm thick) coverslip and observed immediately under the microscope.

ATP depletion, and inhibition of transcription and protein phosphorylation

For ATP-depletion, roots or protoplasts were treated with the respiratory inhibitor sodium azide (Sigma-Aldrich) at 10 mM and the glycolysis inhibitor 2-deoxyglucose (CalBiochem) at 50 mM for 1 hour at room temperature (Brandizzi et al., 2002; Phair and Misteli, 2000). Reversibility of ATP-depletion was determined after washing the sodium-azide- and 2-deoxyglucose-treated roots with MS medium without these inhibitors. ATP-levels were determined with a luciferase-based ATP determination kit according to the manufacturers protocol (catalogue number A22066, Molecular Probes). Viability of protoplasts after ATP-depletion was assayed with Fluorescein diacetate (FDA). Transcription or protein phosphorylation was inhibited by actinomycin D (CalBiochem) at 5 μg ml^{-1} or staurosporine (CalBiochem) at 10 μM for 2 hours. Roots expressing GFP-SR45 or GFP alone were fixed in 2% formaldehyde for 30 minutes.

Confocal microscopy, and FRAP and FLIP analyses

All photobleaching experiments (FRAP and FLIP) were performed with a Zeiss LSM 510 Meta laser scanning microscope using a 63×, N.A. 1.4 oil-immersion apochromate objective. A fixed circular area of 1-μm radius was bleached with 15 full-strength pulses of a 25 mW argon laser (488 nm). The bleaching routine started with four pre-bleach scans, followed by the bleaching scan that lasted for approximately 200 milliseconds. After bleaching, images were taken at the attenuated 0.1-0.5% laser transmission. The first image at the end of bleaching was taken immediately, the rest of the images were taken at a 98-250-millisecond constant interval for 60 seconds or until maximal recovery was reached.

For quantitative FRAP analyses, fluorescence intensity of the bleached area and the entire nucleus was determined using LSM 510 software. Background-corrected intensities were normalized for photobleaching resulting from bleach-pulse and normal scanning according to following equation: $I=I_t/I_0 \times T_0/T_t$, where I is the normalized intensity of the bleached area, T_0, total nuclear intensity before bleach, T_t, total nuclear intensity at time interval t after bleaching, I_0, intensity of the bleached area before bleaching and I_t, intensity of the bleached area at time intervals t after bleaching. The resulting normalized intensity data were fitted to the following exponential models: $I=Y_{max}(1-e^{(-k1\times t)})$, where Ymax is the final level of recovery, t is the time in seconds and k is recovery rate constant. All nonlinear curve fitting and the statistical comparisons were performed in GraphPad Prism 4.0 (http:/www.graphpad.com). Total maximal recovery values represent total mobile population. The immobile fraction was calculated as 1– mobile fraction, with 1 as 100% recovery. D_{eff} values were calculated according to the following formula: $D_{eff}=0.88\times(r^2/4\times t_{1/2})$ (Axelrod et al., 1976), where, r is radius of the bleached area, $t_{1/2}$ is the time when half of the final fluorescence has recovered. The D_{eff} values of GFP alone (29 kDa) and of NLS-GFP-GUS (91 kD) were considered as free diffusion and were used as a reference for comparing changes in the mobility of SR1-YFP and GFP-SR45 and its various deletion mutants. Simulation curves reflecting free diffusions for full-length GFP-SR45 and deletions were constructed using the D_{eff} value of GFP as 15 μm^2 $seconds^{-1}$ and the bleach-spot-radius value as 1.0 μm. The predicted free-diffusion D_{eff} value for GFP-SR45 was calculated from the D_{eff} value of GFP alone, considering that diffusion is inversely proportional to the cubic root of the mass (i.e. $D \alpha M^{-1/3}$) (Sprague et al., 2004).

For FLIP analyses, two nuclei in the same view-field were imaged. In one of these nuclei, a defined area (2 μm diameter) located at one end of the nucleus was bleached at 100% (488-nm laser power with 15 iterations) and imaged. This process was repeated at 5-second intervals until most of the fluorescence in the control nuclei had diminished. The other nucleus was not bleached and was used to normalize for fluorescence intensity. The recorded images were imported into the NIH Image J as stacks, and the fluorescence intensities of the bleached and unbleached areas of the bleached nucleus and of the entire unbleached nucleus were determined and imported into Microsoft Excel. The intensity values were normalized for background bleaching, and plotted against time.

The authors thank D. L. Spector, Cold Spring Harbor Laboratory for providing the SR1-YFP transgenic line; D. Galbraith, The University of Arizona for providing seeds of transgenic lines expressing NLS-GFP-GUS; Irene Day for critically reading the manuscript. We are thankful to Steve Fadul at the light-microscopy facility at the University of Colorado Health Sciences Center, Denver, CO 80262 for help with confocal microscopy. This work was supported by a grant from the Department of Energy (DE-FG02-04ER15556) to ASNR.

References

Abel, S. and Theologis, A. (1994). Transient transformation of Arabidopsis leaf protoplasts: a versatile experimental system to study gene expression. *Plant J.* **5**, 421-427.

Ali, G. S., Golovkin, M. and Reddy, A. S. N. (2003). Nuclear localization and in vivo dynamics of a plant-specific serine/arginine-rich protein. *Plant J.* **36**, 883-893.

Axelrod, D., Koppel, D. E., Schlessinger, J., Elson, E. and Webb, W. W. (1976). Mobility measurement by analysis of fluorescence photobleaching recovery kinetics. *Biophys. J.* **16**, 1055-1069.

Beven, A. F., Simpson, G. G., Brown, J. W. and Shaw, P. J. (1995). The organization of spliceosomal components in the nuclei of higher plants. *J. Cell Sci.* **108**, 509-518.

Boudonck, K., Dolan, L. and Shaw, P. J. (1998). Coiled body numbers in the Arabidopsis root epidermis are regulated by cell type, developmental stage and cell cycle parameters. *J. Cell Sci.* **111**, 3687-3694.

Brandizzi, F., Snapp, E. L., Roberts, A. G., Lippincott-Schwartz, J. and Hawes, C. (2002). Membrane protein transport between the endoplasmic reticulum and the Golgi in tobacco leaves is energy dependent but cytoskeleton independent: evidence from selective photobleaching. *Plant Cell* **14**, 1293-1309.

Caceres, J. F., Misteli, T., Screaton, G. R., Spector, D. L. and Krainer, A. R. (1997). Role of the modular domains of SR proteins in subnuclear localization and alternative splicing specificity. *J. Cell Biol.* **138**, 225-238.

Calapez, A., Pereira, H. M., Calado, A., Braga, J., Rino, J., Carvalho, C., Tavanez, J. P., Wahle, E., Rosa, A. C. and Carmo-Fonseca, M. (2002). The intranuclear mobility of messenger RNA binding proteins is ATP dependent and temperature sensitive. *J. Cell Biol.* **159**, 795-805.

Chen, M., Schwab, R. and Chory, J. (2003). Characterization of the requirements for localization of phytochrome B to nuclear bodies. *Proc. Natl. Acad. Sci. USA* **100**, 14493-14498.

Cokol, M., Nair, R. and Rost, B. (2000). Finding nuclear localization signals. *EMBO Rep.* **1**, 411-415.

Colwill, K., Pawson, T., Andrews, B., Prasad, J., Manley, J. L., Bell, J. C. and Duncan, P. I. (1996). The Clk/Sty protein kinase phosphorylates SR splicing factors and regulates their intranuclear distribution. *EMBO J.* **15**, 265-275.

Docquier, S., Tillemans, V., Deltour, R. and Motte, P. (2004). Nuclear bodies and compartmentalization of pre-mRNA splicing factors in higher plants. *Chromosoma* **112**, 255-266.

Dye, B. T. and Patton, J. G. (2001). An RNA recognition motif (RRM) is required for the localization of PTB-associated splicing factor (PSF) to subnuclear speckles. *Exp. Cell Res.* **263**, 131-144.

Fang, Y., Hearn, S. and Spector, D. L. (2004). Tissue-specific expression and dynamic organization of SR splicing factors in Arabidopsis. *Mol. Biol. Cell* **15**, 2664-2673.

Golovkin, M. and Reddy, A. S. N. (1999). An SC35-like protein and a novel serine/arginine-rich protein interact with Arabidopsis U1-70K protein. *J. Biol. Chem.* **274**, 36428-36438.

Graveley, B. R. (2000). Sorting out the complexity of SR protein functions. *RNA* **6**, 1197-1211.

Hedley, M. L., Amrein, H. and Maniatis, T. (1995). An amino acid sequence motif sufficient for subnuclear localization of an arginine/serine-rich splicing factor. *Proc. Natl. Acad. Sci. USA* **92**, 11524-11528.

Huang, Y. and Steitz, J. A. (2005). SRprises along a messenger's journey. *Mol. Cell* **17**, 613-615.

Kalyna, M. and Barta, A. (2004). A plethora of plant serine/arginine-rich proteins: redundancy or evolution of novel gene functions? *Biochem. Soc. Trans.* **32**, 561-564.

Kalyna, M., Lopato, S. and Barta, A. (2003). Ectopic expression of atRSZ33 reveals its function in splicing and causes pleiotropic changes in development. *Mol. Biol. Cell* **14**, 3565-3577.

Kircher, S., Gil, P., Kozma-Bognar, L., Fejes, E., Speth, V., Husselstein-Muller, T., Bauer, D., Adam, E., Schafer, E. and Nagy, F. (2002). Nucleocytoplasmic partitioning of the plant photoreceptors phytochrome A, B, C, D, and E is regulated differentially by light and exhibits a diurnal rhythm. *Plant Cell* **14**, 1541-1555.

Kruhlak, M. J., Lever, M. A., Fischle, W., Verdin, E., Bazett-Jones, D. P. and Hendzel, M. J. (2000). Reduced mobility of the alternate splicing factor (ASF) through the nucleoplasm and steady state speckle compartments. *J. Cell Biol.* **150**, 41-51.

Lamond, A. I. and Earnshaw, W. C. (1998). Structure and function in the nucleus. *Science* **280**, 547-553.

Lamond, A. I. and Spector, D. L. (2003). Nuclear speckles: a model for nuclear organelles. *Nat. Rev. Mol. Cell Biol.* **4**, 605-612.

Lazar, G., Schaal, T., Maniatis, T. and Goodman, H. M. (1995). Identification of a plant serine-arginine-rich protein similar to the mammalian splicing factor SF2/ASF. *Proc. Natl. Acad. Sci. USA* **92**, 7672-7676.

Lewis, J. D. and Tollervey, D. (2000). Like attracts like: getting RNA processing together in the nucleus. *Science* **288**, 1385-1389.

Li, H. and Bingham, P. M. (1991). Arginine/serine-rich domains of the su(wa) and tra RNA processing regulators target proteins to a subnuclear compartment implicated in splicing. *Cell* **67**, 335-342.

Lopato, S., Gattoni, R., Fabini, G., Stevenin, J. and Barta, A. (1999a). A novel family of plant splicing factors with a Zn knuckle motif: examination of RNA binding and splicing activities. *Plant Mol. Biol.* **39**, 761-773.

Lopato, S., Kalyna, M., Dorner, S., Kobayashi, R., Krainer, A. R. and Barta, A. (1999b). atSRp30, one of two SF2/ASF-like proteins from Arabidopsis thaliana, regulates splicing of specific plant genes. *Genes Dev.* **13**, 987-1001.

Lorkovic, Z. J. and Barta, A. (2002). Genome analysis: RNA recognition motif (RRM) and K homology (KH) domain RNA-binding proteins from the flowering plant *Arabidopsis thaliana*. *Nucleic Acids Res.* **30**, 623-635.

Lorkovic, Z. J. and Barta, A. (2004). Compartmentalization of the splicing machinery in plant cell nuclei. *Trends Plant Sci.* **9**, 565-568.

Lorkovic, Z. J., Wieczorek Kirk, D. A., Lambermon, M. H. and Filipowicz, W. (2000). Pre-mRNA splicing in higher plants. *Trends Plant Sci.* **5**, 160-167.

Lorkovic, Z. J., Hilscher, J. and Barta, A. (2004). Use of fluorescent protein tags to study nuclear organization of the spliceosomal machinery in transiently transformed living plant cells. *Mol. Biol. Cell* **15**, 3233-3243.

Mintz, P. J., Patterson, S. D., Neuwald, A. F., Spahr, C. S. and Spector, D. L. (1999). Purification and biochemical characterization of interchromatin granule clusters. *EMBO J.* **18**, 4308-4320.

Misteli, T. (2000). Cell biology of transcription and pre-mRNA splicing: nuclear architecture meets nuclear function. *J. Cell Sci.* **113**, 1841-1849.

Misteli, T. (2001). Protein dynamics: implications for nuclear architecture and gene expression. *Science* **291**, 843-847.

Misteli, T. and Spector, D. L. (1999). RNA polymerase II targets pre-mRNA splicing factors to transcription sites *in vivo*. *Mol. Cell* **3**, 697-705.

Misteli, T., Caceres, J. F. and Spector, D. L. (1997). The dynamics of a pre-mRNA splicing factor in living cells. *Nature* **387**, 523-527.

Misteli, T., Caceres, J. F., Clement, J. Q., Krainer, A. R., Wilkinson, M. F. and Spector, D. L. (1998). Serine phosphorylation of SR proteins is required for their recruitment to sites of transcription in vivo. *J. Cell Biol.* **143**, 297-307.

Molenaar, C., Abdulle, A., Gena, A., Tanke, H. J. and Dirks, R. W. (2004). Poly(A)+ RNAs roam the cell nucleus and pass through speckle domains in transcriptionally active and inactive cells. *J. Cell Biol.* **165**, 191-202.

Phair, R. D. and Misteli, T. (2000). High mobility of proteins in the mammalian cell nucleus. *Nature* **404**, 604-609.

Reddy, A. S. (2004). Plant serine/arginine-rich proteins and their role in pre-mRNA splicing. *Trends Plant Sci.* **9**, 541-547.

Reddy, A. S. N. (2001). Nuclear pre-mRNA splicing in plants. *Crit. Rev. Plant Sci.* **20**, 523-571.

Sacco-Bubulya, P. and Spector, D. L. (2002). Disassembly of interchromatin granule clusters alters the coordination of transcription and pre-mRNA splicing. *J. Cell Biol.* **156**, 425-436.

Saitoh, N., Spahr, C. S., Patterson, S. D., Bubulya, P., Neuwald, A. F. and Spector, D. L. (2004). Proteomic analysis of interchromatin granule clusters. *Mol. Biol. Cell* **15**, 3876-3890.

Sanford, J. R. and Bruzik, J. P. (1999). Developmental regulation of SR protein phosphorylation and activity. *Genes Dev.* **13**, 1513-1518.

Shav-Tal, Y., Darzacq, X., Shenoy, S. M., Fusco, D., Janicki, S. M., Spector, D. L. and Singer, R. H. (2004). Dynamics of single mRNPs in nuclei of living cells. *Science* **304**, 1797-1800.

Shaw, P. J. and Brown, J. W. (2004). Plant nuclear bodies. *Curr. Opin. Plant Biol.* **7**, 614-620.

Spector, D. L. (2001). Nuclear domains. *J. Cell Sci.* **114**, 2891-2893.

Sprague, B. L., Pego, R. L., Stavreva, D. A. and McNally, J. G. (2004). Analysis of binding reactions by fluorescence recovery after photobleaching. *Biophys. J.* **86**, 3473-3495.

Tao, L. Z., Cheung, A. Y., Nibau, C. and Wu, H. M. (2005). RAC GTPases in tobacco and Arabidopsis mediate auxin-induced formation of proteolytically active nuclear protein bodies that contain AUX/IAA proteins. *Plant Cell* **17**, 2369-2383.

Tillemans, V., Dispa, L., Remacle, C., Collinge, M. and Motte, P. (2005). Functional distribution and dynamics of Arabidopsis SR splicing factors in living plant cells. *Plant J.* **41**, 567-582.

Vargas, D. Y., Raj, A., Marras, S. A., Kramer, F. R. and Tyagi, S. (2005). Mechanism of mRNA transport in the nucleus. *Proc. Natl. Acad. Sci. USA* **102**, 17008-17013.

Xiao, S. H. and Manley, J. L. (1997). Phosphorylation of the ASF/SF2 RS domain affects both protein-protein and protein-RNA interactions and is necessary for splicing. *Genes Dev.* **11**, 334-344.

Zeng, C., Kim, E., Warren, S. L. and Berget, S. M. (1997). Dynamic relocation of transcription and splicing factors dependent upon transcriptional activity. *EMBO J.* **16**, 1401-1412.